Assessment of soil liquefaction by EQUATERRE Cyclic static penetrometer.

Hamid Hosseini Sadrabadi[*, **]

**3sr lab, Univ. Grenoble Alpes; **Equaterre company, Grenoble, France.*

e-mail : h.hosseini@equaterre-geotechique.fr

Bruno Chareyre[1], Luc Sibille[2], Christophe Dano[3] , Ankit Sharma[4]

3sr lab, Univ. Grenoble Alpes , Grenoble, France.

e-mail[1]: bruno.chareyre@3sr-grenoble.fr,

e-mail[2] : luc.sibille@3sr-grenoble.fr,

e-mail[3]: christophe.dano@3sr-grenoble.fr,

e-mail[4]: ankit.sharma@3sr-grenoble.fr

Pierre Riegel[**]

Equaterre Company, Meythet, France.

e-mail: pierreriegel@yahoo.fr

ABSTRACT: This project aims at improving the interpretation of the CPT (without measurement of pore pressure) for the recognition of liquefiable soils. We present numerical and experimental approaches exploring the possibility of using cyclic loading data from the tip of a CPT to evaluate the liquefaction potential of the soil. The experimental part is based on CPTU and cyclic CPT tests developed by Equaterre performed in a calibration chamber. The numerical model of the penetrometer is based on a coupling between the discrete element method to describe the solid phase and a finite volume method defined at the pore scale to solve the dynamics of the pore fluid in saturated conditions. The experimental and numerical results are analyzed in a complementary way to highlight how this information could be used to evaluate the liquefaction potential of the soil.

Keywords: cyclic CPT; calibration chamber; DEM; fluid-solid coupling; soil liquefaction.

1. Introduction

The cone penetration test (CPT) is commonly used for in-situ investigation of sub-surface soil layers. Empirical correlations from CPT tests or more advanced penetration tests like CPTu allows evaluating the liquefaction potential of soils (Robertson et Wride, 1998). In this paper, both numerical and experimental approaches, investigating the possibility to use data resulting from a cyclic loading of the cone tip, are presented to evaluate the liquefaction potential. The experimental part is based on a comparison between standard CPTu tests and cyclic cone penetration tests performed in a calibration chamber using an original cyclic CPT device specifically developed by Equaterre Company (Riegel, 2017).

The numerical model of the CPT associates the discrete element method which describes the solid phase, and a finite volume method defined at the pore scale (Catalano et al., 2014), to solve the seepage flow in saturated conditions. In addition to the tip resistance, this model gives access to the fields of stresses, displacements, pore pressure and fluid velocity in the whole soil volume.

Experimental and numerical results are analyzed in a complementary way to highlight: first, the key information which can be provided by a cyclic CPT in typically loose and dense fine sands and, second, how this information could be used to evaluate the liquefaction potential of a soil.

2. Cyclic cone penetration test

For more than 20 years, Equaterre-group has monitored soil investigation campaigns, in particular in post-glacial lands (moraine ...). The precedence of the penetrometer practice has led to the use of a double measure by a "Gouda" tip (Figure 1), which consists in measuring successively the tip resistance at a driving speed of 2 cm.s^{-1} ($Q_c^{2cm/s}$) and the stationary force on the tip measured after stopping at a particular position (Q_c^{stop}). By analogy, the loading of the soil by a foundation is closer to the measurement at standstill (Q_c^{stop}) than the measurement while the tip is moving ($Q_c^{2cm/s}$), more significantly in soils of low permeability where CPT driving is effected by pore pressure effects to a greater effect. (Hosseini et al, 2016; Riegel et Hosseini, 2014). The so-called double measure quantifies the difference $\Delta q_c = Q_c^{2cm/s} - Q_c^{stop}$.

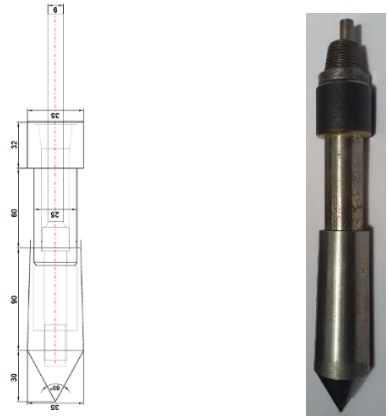

Figure 1. Gouda tip

The values of Δq_c vary considerably with the type of soil. Experience also suggests a specific response in the context of liquefiable materials.

After assessment of possible liquefiable soils with the *double measure* method, the liquefaction potential is assessed by performing a direct loading with a cyclic CPT. The cyclic CPT device (Riegel, 2017) includes an innovative additional module to impose a cyclic loading directly to the cone tip. By this way, the direct reaction of the soil against the cyclic loading can be monitored. It can be used in either a controlled-force mode or in a controlled-displacement mode. The frequency can be chosen from 0.5 to 5 Hz. In this study, it was set to 1 Hz. For the sake of simplicity and robustness of the cyclic CPT device, the latter does not include a pore pressure cell.

3. Calibration chamber testing program

This section aims to present the experimental set-up and the operative steps performed during CPT testing programme in the large 3SR Calibration Chamber. CPTu and cyclic Equaterre CPT tests were performed in fine siliceous sand specimens in two different density states (subsequently referred to loose and medium dense states).

3.1. Tested material

GA39 Fontainebleau sand (G_s = 2.65, e_{min} = 0.56, e_{max} = 1.01) was selected because of its fineness

(d_{50}=110µm), its uniformity (C_u=1.2) (Figure 2) that makes it prone to liquefaction in relevant conditions. Medium dense specimens (D_R≈55%) were reconstituted by dry tamping of 100 kg sand layers, whereas loose specimens (D_R < 40%) were obtained by pluviating the sand in water with a small drop height.

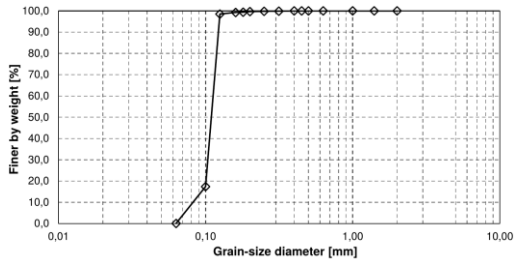

Figure 2. Particle size distribution of Fontainebleau GA39 sand

3.2. Calibration chamber tests equipment

The main features of Calibration Chamber tests are represented by the simultaneous possibility to create large soil samples with specific state parameters, to control independently different boundary conditions and to follow stress paths typical of in-situ tests. In the present case, the lateral boundary condition is similar to oedometric conditions, e.g. no lateral displacement.

3.2.1. The large 3SR Calibration Chamber

The 3SR Calibration Chamber (Silva, 2014) is schematically illustrated in Figure 3. It consists of three cylindrical rigid steel sections of 0.5 m height and 1.20 m internal diameter. The three steel sections are assembled together by metal bolts up to a total height of 1.5 m. A pressurized membrane exerts a vertical stress on the top surface, just below the top cap fitted with a central hole, allowing the driving of penetrometers for instance.

An unexpected leakage in the lateral ring resulted in an incomplete saturation (Figure 4) of the specimens, as shown by the pore water measurements during CPTu driving. Therefore, only tests done in the fully saturated zone, in the bottom part of the specimens, are presented.

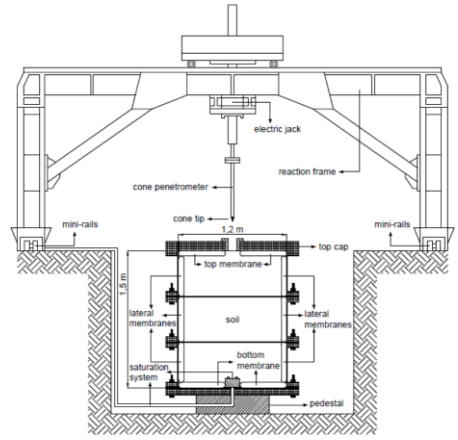

Figure 3. Grenoble Laboratory 3SR Calibration Chamber equipment.

3.3. Calibration Chamber CPT test

CPTu tests were first carried out on specimens vertically consolidated at a vertical stress of 100 kPa to validate the liquefaction potential of the sand specimens, following Robertson's chart. Then, a second specimen was tested in the same conditions (medium dense or loose) using the Equaterre cyclic CPT. The medium dense specimen was consolidated at a vertical stress of 100 kPa, whereas no confinement was applied in the loose specimen, still to favour liquefaction.

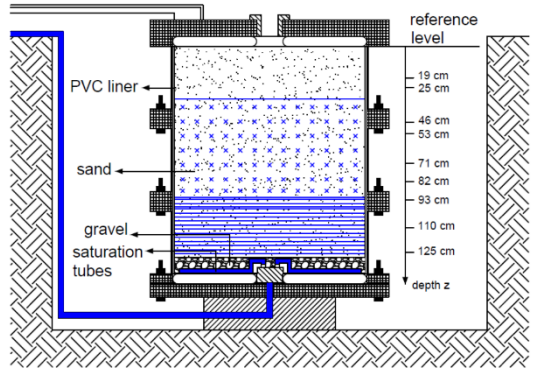

Figure 4. Saturation condition in Calibration Chamber

3.3.1. CPTu test results

The two series of CPTu in medium dense and loose sands were performed with a double measure of tip resistance ($Q_c^{2cm/s}$) and (Q_c^{stop}) each 10 cm. Pore pressure was also recorded. Values of tip resistance validate the liquefiable nature of the loose specimens and

the non-liquefiable nature of the medium dense specimen. In figure 5 the dilatant behaviour of dense sand with reduction in pore pressure during driving and pressure recovery during stop is observed. On the contrary, for loose sands, the contractive behaviour induces an increase in pore pressure during driving and a dissipation during stop (Figure 6). Evolution of pore pressure seen experimentally will be confirmed in the subsequent numerical simulations.

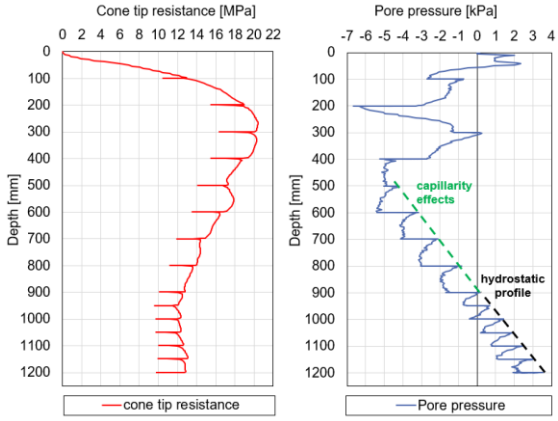

Figure 5. Medium dense sand tip resistance and pore pressure.

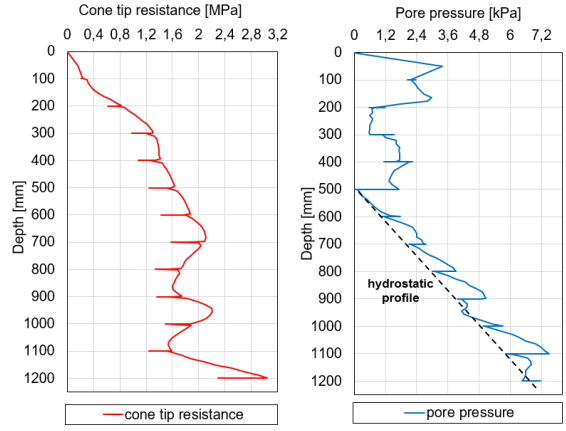

Figure 6. Loose sand tip resistance and pore pressure.

3.3.2. Cyclic tests with Equaterre's CPT

The cyclic tests with Equaterre's CPT device (without pore pressure measurements) consists in a first monotonic driving up to a specified tip load. Then the tip is maintained in a fixed position for one minute, at the end of which the cyclic loading is applied between two prescribed values of the tip load (Figure7).

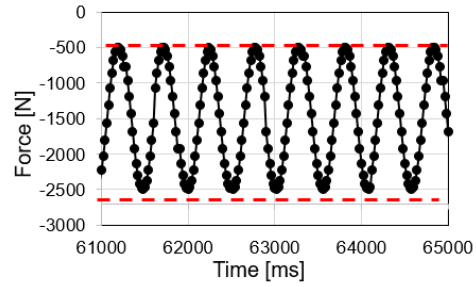

Figure 7. Controlled force loading for the dense sand specimen.

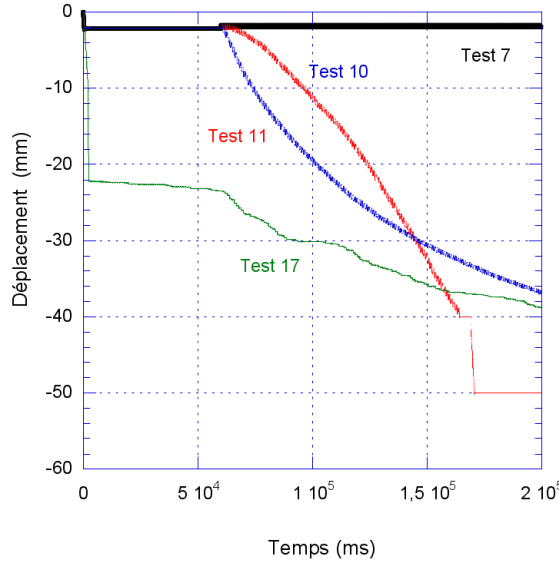

Figure 8. Response cyclic CPT in dense and loose sands.

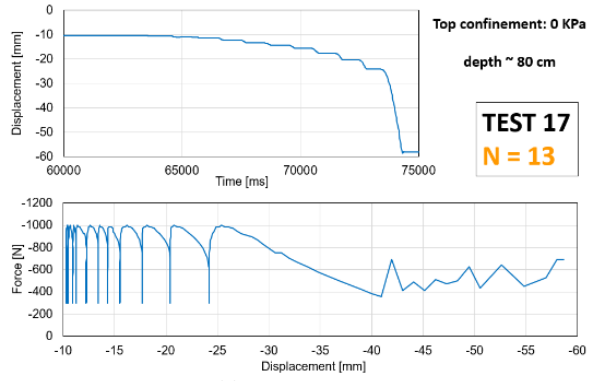

Figure 9. Evolution of force and displacement in loose sand.

During cyclic loading, dense specimens do not exhibit any significant displacements of the tip on application of cyclic load as is seen is Test 7 in Figure 8. On the contrary, in loose sand, accumulation of vertical displacements of the tip occurred as is seen in Test 17 up to a sudden collapse after 13 cycles, which may be interpreted as the result of the soil liquefaction below the CPT tip (Figures 8 and 9).

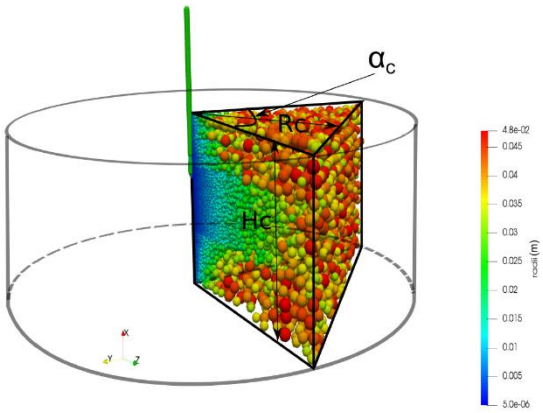

Figure 10. Geometry of the numerical model of the calibration chamber.

4. Numerical fluid-solid penetration model

4.1. DEM-PFV method

The 3D numerical model is based on the combination of the Discrete Element Method (DEM) to describe the mechanical behavior of the solid soil skeleton with a pore scale finite volume (PFV) method tosolve the pore fluid dynamics (Catalano et al., 2014). The particles are spheres interacting through elastic-frictional contacts. Rolling friction is included in addition to sliding friction in order to reflect the role of particle angularity and shape indirectly. The fluid flow is supposed Stokesian and incompressible (Darcy flow). The fluid is solved on a tetrahedral mesh advected in a Lagrangian way to follow particle motion, following the PFV method described in Catalano et al. (2014) and Chareyre et al. (2011). The application of the PFV solver gives the field of pore pressure at every instant, from which the forces exerted by the fluid on the solid grains are deduced and integrated into the DEM cycle. The model includes six mechanical parameters: normal(k_n), tangential(k_s) and rolling(k_r) contact stiffnesses, contact(φ_c) and rolling(η_r) friction coefficients, and permeability(k). Note that the model presented here differs from Catalano et al. (2014) by the setting of permeability. The original model predicts permeability as a function of particle size. The current model takes macroscopic permeability as an input parameter directly. An adaptation that was necessary due to the particle coarsening method presented hereafter – which would have caused a gradient of Darcy permeability across the chamber.

4.2. Calibration chamber model.

Thanks to the symmetry of revolution of the calibration chamber, only a quarter of the real geometry has been represented in the numerical simulations to limit the computational cost (Hosseini et al., 2016). The model has the shape of a prism. One of the edges of the prism coincides with the axis of symmetry, which is also the axis of the penetrometer (Figure 10). The boundaries of the prism consist of fixed rigid walls (zero friction between the particles and the walls) and impervious to the fluid. The ratio R_d between the radius of the tip (R=0.25m) and the radius of the calibration chamber(Rc=1.5m) was set at 60 in order to limit the boundary effects on the tip resistance and height of calibration camber (Hc) is 1.3m. Finally, to optimize again the computation cost, a coarsening of the particle size distribution with distance from the tip was implemented (Figure 11). By filling remote zones with bigger particles computational power can be spend on computing more accurately the soil-tip interactions with fine particles.

The granular assembly is initially generated in the form of a random loose cloud of non-contacting particles, with a gradient in size distribution reflecting the distance from the tip, and compacted by a sphere growing procedure preserving the shape of the size distribution. By tuning contact friction or adhesion during the compaction phase two different initial states were generated, dense and loose respectively (adhesion is removed, and contact friction is restored to an independent value after the compaction process). The porosities of the dense and loose assemblies are 0.35 and 0.45 respectively. The permeability(k) is set at 10^{-7} m/s. Such a relatively low numerical permeability value has been chosen in order to emphasize the effect of the pore pressure in the numerical model.

The ratio of tip diameter to particle diameter is 18 near the tip. Initial confinement is applied to the granular assembly, prior to the driving of the penetrometer, reflecting the effect of the depth.

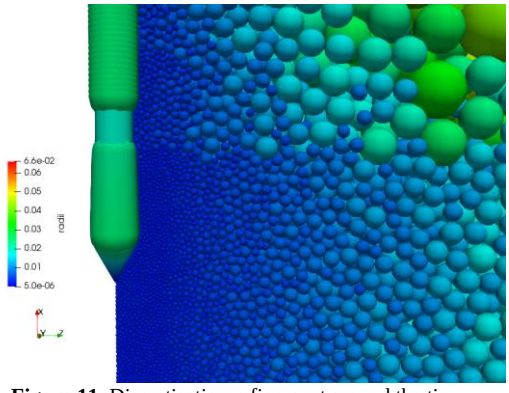

Figure 11. Discretisation refinement around the tip.

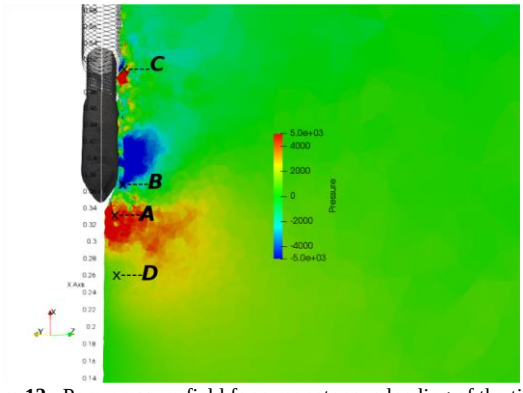

Figure 12. Pore-pressure field for a monotonous loading of the tip in a loose granular assembly.

4.3. Monotonous loading

A CPT test is simulated at a constant penetration rate under an initial confinement stress of 100 kPa (effective stress). The driving speed is 1 m/s (monotonous loading). This penetration rate is higher than in situ conditions, however a parametric study showed that, for the numerical model, the effect of the driving speed on Q_c (tip resistance) was negligible up to this penetration rate (but not beyond).

4.3.1. Pore pressure characterization

The pore pressure is followed at four points (A, B, C and D, defined in Figure 12), relative to the position of the tip and moving with it.

Figures 13 and 14 present the pore pressure evolution in the dense and loose sands with the tip displacement. As observed with the CPTu test in the calibration chamber, a reduction of the pore pressure in the nearest zone of the tip (points A & B) is simulated for the dense granular assembly, in agreement with the dilatant behaviour of dense sands. For the loose granular assembly, the increase of the pore pressure, relative to the contractant behaviour of the soil, is also found numerically around the tip. Point B is an exception where the pressure, even if it is higher than in the dense case, is not always positive; this is the consequence of local deformation mechanisms around the tip.

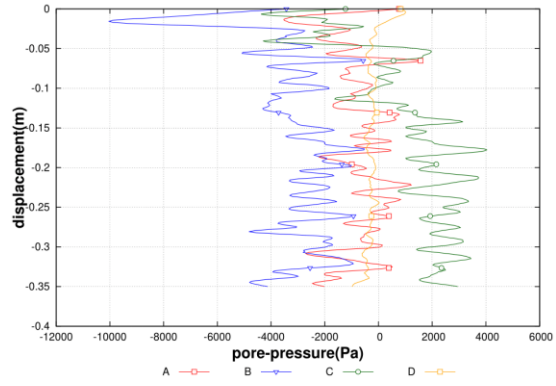

Figure 13. Pore pressure in dense assembly.

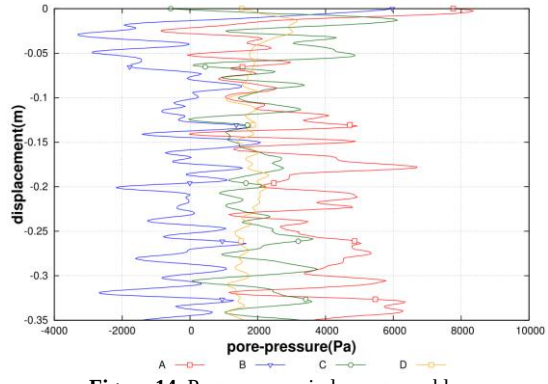

Figure 14. Pore pressure in loose assembly.

4.4. Cyclic loading.

A cyclic loading of the tip of the penetrometer has been simulated in a similar way to the Equaterre cyclic CPT performed in the calibration chamber. After driving the tip monotonously until a given depth, the cyclic loading of the tip is controlled by imposing the tip stress between two prescribed values (both lower than the tip resistance) with a period T = 0.004s. This period is relatively low with respect to the period used in the calibration chamber. It has been chosen to limit the computation cost by limiting the physical time to be simulated. A parametric study performed for a period from 0.004s to 0.4s showed that the effect on the tip resistance is negligible with current settings. This parametric study needs to be completed. Figures 15 and 16 present the position of tip and evolution of pore pressure with cyclic loading.

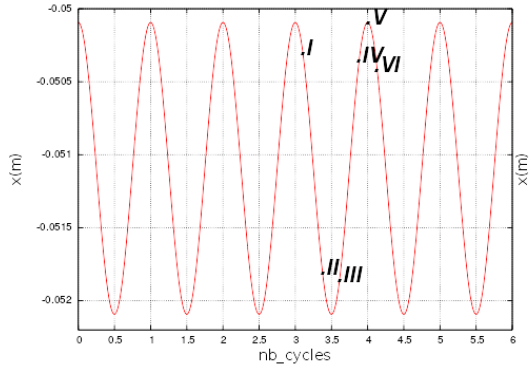

Figure 15. Cyclic loading position

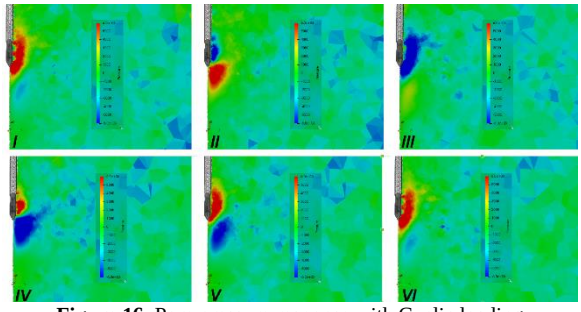

Figure 16. Pore pressure response with Cyclic loading

Figures 13 &14 present the evolution of the tip displacement in dense and loose granular assemblies respectively. The results are in good agreement with the ones obtained from the calibration chamber. The numerical model has not been calibrated so far on the mechanical behaviour of the sand used in the calibration chamber. Consequently, we focus on the general trend of the numerical model and the comparison is only qualitative. The vertical displacement of the tip is almost reversible for the dense assembly whereas an accumulation of the displacement is obtained in the loose assembly. The reversible and irreversible behaviours of the soil-tip system, for dense and loose assemblies respectively, are highlighted in Figures 17 and 18, showing the tip stress-displacement relation.

No collapse of the soil below the tip was observed numerically for the loose assembly, contrary to the test in the calibration chamber. This may be due to the too low number of cycles simulated numerically. Responses of the numerical model over a larger number of cycles still need to be investigated.

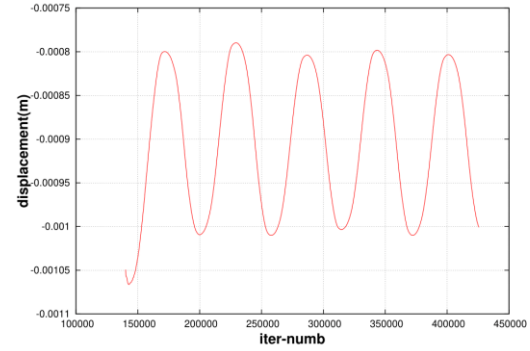

Figure 17. Tip displacement in the dense assembly for a cyclic stress control loading.

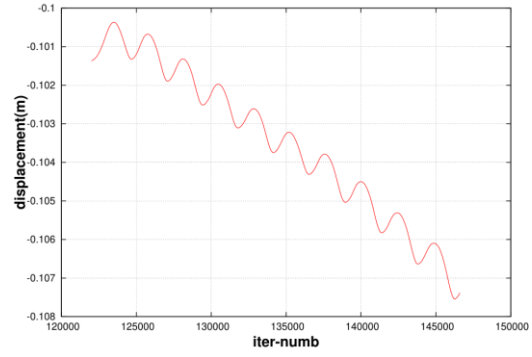

Figure 18. Tip displacement in the loose assembly for a cyclic stress control loading.

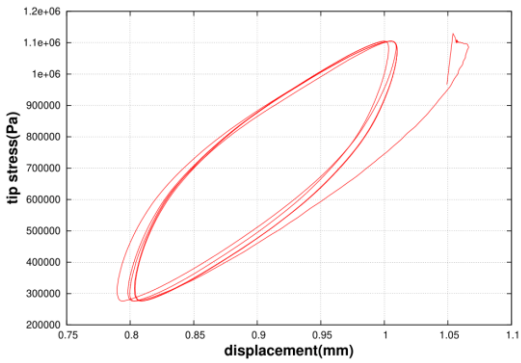

Figure 19. Evolution of tip stress and displacement in the dense assembly.

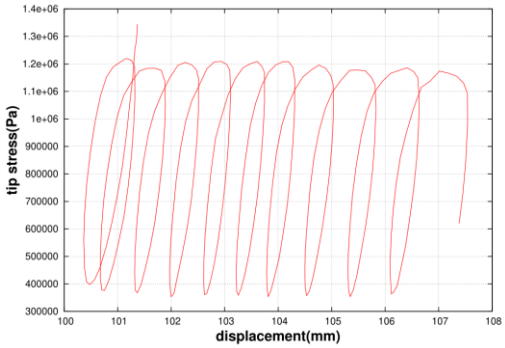

Figure 20. Evolution of tip stress and displacement in the loose assembly.

5. Conclusions

Preliminary tests in a large calibration chamber, coupled with numerical simulations performed at the particle scale, aimed at developing and validating the expected performances of an original cyclic CPT.

The experimental and numerical results show that the Equaterre cyclic CPT could be a promising tool to assess the potential of liquefaction of sandy soils, without the direct measurement of the pore pressure as in a CPTu. In particular, an accumulation of irreversible vertical displacements of the tip is observed during the force control cycles in the loose fine sand, eventually evolving, in the calibration chamber, toward a loss of controllability of the tip loading when soil liquefaction is expected to occur.

The results presented in this paper give a first insight about how the data from the cyclic CPT could be used to characterize the encountered soil layers. Nevertheless, they need to be confirmed and complete by more thorough tests in calibration chamber, numerical simulations, but also field tests in real conditions.

6. ACKNOWLEDGEMENTS

This work has been partially supported by the LabEx Tec 21 (Investissement d'Avenir – grant agreement no ANR-11-LABX-0030).

7. References

[1] Butlanska, J. 2014. Cone penetration test in a virtual calibration chamber. PhD Thesis, Universitat Politécnica de Catalunya.

[2] Catalano, E., Chareyre, B., Barthélémy, E. 2014. Pore-scale modeling of fluid-particles interaction and emerging poromechanical effects. International Journal for Numerical and Analytical Methods in Geomechanics 38(1), 51–71.

[3] Chareyre, B., Cortis, A., Catalano E., Barthélemy, E. 2011. Pore-scale modeling of viscous flow and induced forces in dense sphere packings. Transport in Porous Media 92(2), 473–493.

[4] DTU, 13.2.1992.AFNOR , fondations profondes pour le bâtiment, pp.66.

[5] Hosseini, S.H., Chareyre, B., Sibille, L., Riegel, P. 2016. Identification des sols liquéfiables par pénétromètre statique: principe et modélisation numérique. JNGG 2016, 6-8 juillet 2016, Nancy. https://jngg2016.science conf.org/78564/document.

[6] Riegel, P. 2017. Pénétromètre statique pour l'évaluation du caractère liquéfiable d'un sol et procédés associés. Dépôt de brevet FA841687. 18 août 2017.

[7] Riegel, P., Hosseini, S.H. (2014). L'usage du pénetromètre statique dans l'approche des tassements sous ouvrage. Retour d'expérience en milieu compressible par suivi du comportement du sol sous remblai de préchargement validité et amélioration des corrélations modules/qc. JNGG 2014, 8-9 juillet 2014, Beauvais.

[8] Robertson, P. K., & Wride, C. E. (1998). Evaluating cyclic liquefaction potential using the cone penetration test. Canadian Geotechnical Journal, 35(3), 442-459.

[9] Silva, M. 2014. Experimental study of ageing and axial cyclic loading effect on shaft friction along driven piles in sand. Ph.D. Thesis, University of Grenoble.